8. G. Giannone *et al.*, *Cell* **116**, 431 (2004).
9. N. Watanabe, T. J. Mitchison, *Science* **295**, 1083 (2002).
10. G. Danuser, R. Oldenbourg, *Biophys. J.* **79**, 191 (2000).
11. T. M. Svitkina *et al.*, *J. Cell Biol.* **160**, 409 (2003).
12. A. Mallavarapu, T. Mitchison, *J. Cell Biol.* **146**, 1097 (1999).
13. J. A. Theriot, T. J. Mitchison, L. G. Tilney, D. A. Portnoy, *Nature* **357**, 257 (1992).
14. G. H. Patterson, J. Lippincott-Schwartz, *Science* **297**, 1873 (2002).
15. Materials and methods are available as supporting material on *Science* Online.
16. T. Nishizaka, Q. Shi, M. P. Sheetz, *Proc. Natl. Acad. Sci. U.S.A.* **97**, 692 (2000).
17. C. G. Galbraith, K. M. Yamada, M. P. Sheetz, *J. Cell Biol.* **159**, 695 (2002).
18. W. B. Kiosses, S. J. Shattil, N. Pampori, M. A. Schwartz, *Nat. Cell Biol.* **3**, 316 (2001).
19. D. P. Felsenfeld, P. L. Schwartzberg, A. Venegas, R. Tse, M. P. Sheetz, *Nat. Cell Biol.* **1**, 200 (1999).
20. N. A. Medeiros, D. T. Burnette, P. Forscher, *Nat. Cell Biol.* **8**, 215 (2006).
21. A. Horwitz, K. Duggan, C. Buck, M. C. Beckerle, K. Burridge, *Nature* **320**, 531 (1986).
22. J. A. DePasquale, C. S. Izzard, *J. Cell Biol.* **113**, 1351 (1991).
23. C. A. Otey, F. M. Pavalko, K. Burridge, *J. Cell Biol.* **111**, 721 (1990).
24. D. M. Suter, P. Forscher, *J. Cell Biol.* **155**, 427 (2001).
25. D. Bentley, A. Toroian-Raymond, *Nature* **323**, 712 (1986).
26. D. Choquet, D. P. Felsenfeld, M. P. Sheetz, *Cell* **88**, 39 (1997).
27. T. P. Loisel, R. Boujemaa, D. Pantaloni, M. F. Carlier, *Nature* **401**, 613 (1999).
28. We thank C. Smith and T. Reese for suggestions on the experiments and manuscript and M. Sheetz for use of optical trap data collected by C.G.G. while in his laboratory. For use of the laser scanning microscopes, we thank the National Institute of Neurological Disorders and Stroke (NINDS) Light Imaging Facility for the LSM 510 (VIS/405) and Carl Zeiss, Inc., for the LSM 5 LIVE and LSM 5 DUO. We also thank Z. Iwinski for confocal software; E. Shumsky, R. Engelmann, and S. Tille for assistance; G. Patterson and J. Lippincott-Schwartz for PaGFP and discussions; and M. Hoffman for assistance with reverse transcription–polymerase chain reaction studies. Reagents provided by R. Tsien (mRFP), J. Wehland (EGFP-VASP), and S. Yamada (human foreskin fibroblasts). Support provided by the intramural research programs of NINDS and National Institute of Dental and Craniofacial Research, NIH.

Supporting Online Material

www.sciencemag.org/cgi/content/full/315/5814/992/DC1
Materials and Methods
Figs. S1 to S5
References
Movies S1 to S4

2 November 2006; accepted 5 January 2007
10.1126/science.1137904

Maplike Representation of Celestial *E*-Vector Orientations in the Brain of an Insect

Stanley Heinze and Uwe Homberg*

For many insects, the polarization pattern of the blue sky serves as a compass cue for spatial navigation. *E*-vector orientations are detected by photoreceptors in a dorsal rim area of the eye. Polarized-light signals from both eyes are finally integrated in the central complex, a brain area consisting of two subunits, the protocerebral bridge and the central body. Here we show that a topographic representation of zenithal *E*-vector orientations underlies the columnar organization of the protocerebral bridge in a locust. The maplike arrangement is highly suited to signal head orientation under the open sky.

Many animals, including birds, fishes, cephalopods, and arthropods, share the ability to perceive linearly polarized light (*1*, *2*). The plane of polarization (*E*-vector) varies systematically across the blue sky and depends on the Sun's position. For a variety of insects this pattern has been shown to guide spatial orientation (*2*). In locusts, polarotactic orientation depends on a specialized part of the compound eye, the dorsal rim area (*3*), and involves several central processing stages, including the central complex (*4*–*7*). The central complex (CC) is a group of neuropils spanning the midline of the insect brain. Substructures are the protocerebral bridge (PB) and the upper and lower divisions of the central body. An outstanding anatomical feature of the CC is its regular and highly sophisticated internal neuroarchitecture (*8*–*10*). In simplified terms, it consists of stacks of arrays, each composed of a linear arrangement of 16 columns with topographic interhemispheric connections between columns both within and between different arrays. Hypotheses on the functional roles of the CC range from a control center for motor coordination (*11*) to a recently demonstrated involvement in visual pattern learning and recognition (*12*). In the locust, several cell types of the CC are sensitive to the orientation of zenithal *E*-vectors (*5*), but the correspondence of cell morphology and *E*-vector tuning has remained obscure. In this study, we have used intracellular recordings combined with dye injections to analyze *E*-vector tuning in CC neurons of the locust with columnar arborization domains.

Two major classes of polarization-sensitive (POL) neurons were encountered regularly when we recorded from CC neurons: (i) a particular type of tangential neuron of the PB and (ii) several types of columnar neurons. Tangential neurons of the PB, termed here TB1 neurons, have not been described previously in the locust or any other insect. A total number of 18 of these cells were analyzed. Their morphology was revealed by iontophoretic tracer injection, histological processing, and camera lucida reconstruction (*13*). TB1 neurons provide a connection between a posterior brain region, the posterior optic tubercle, and the PB (Fig. 1, A and B). Each TB1 neuron had two domains of varicose and, thus, putatively presynaptic arborizations confined to a single column in each hemisphere of the PB. When PB columns are numbered as L1 (lateralmost column in the left hemisphere of the PB) to L8 (most medial column in the left hemisphere) and, accordingly, from R1 to R8 in the right hemisphere of the bridge, TB1 neurons with varicose ramifications in columns R1/L8, R2/L7, R4/L5, R5/L4, R6/L3, and R7/L2 were encountered. Varicose processes were always eight columns apart, with processes ipsilaterally in one of the four outer columns and contralaterally in one of the four inner columns (Fig. 1E). The columns neighboring those with varicose processes were free of ramifications, and six to eight other columns were invaded with fine, smooth arborizations. Furthermore, all TB1 neurons had varicose arborizations in the posterior optic tubercle, a brain area connected to a small neuropil in the optic lobe, the accessory medulla (*14*).

The pattern of varicose arborizations in the PB corresponded to physiological properties of the TB1 neurons. For intracellular recordings, the animals were fixed in the recording setup and stimulated from the zenith with a rotating *E*-vector. Recordings were obtained from their main neurite in the PB. Each TB1 neuron showed polarization opponency, i.e., *E*-vector orientations leading to an increase in spiking activity (excitation) were oriented perpendicularly to *E*-vectors, leading to a decrease in spiking activity (inhibition) (Fig. 1, C and D). The *E*-vector tuning (*E*-vector orientation resulting in maximum excitation, Φ_{max}) was determined for each neuron by circular statistics [Rayleigh test (*15*)]. *E*-vector tuning of TB1 neurons showed a linear relation to the position of their varicose ramifications in the PB (Fig. 1F). Thereby, a range of Φ_{max} tunings of 182° ± 71° extends through the eight columns of each hemisphere of the PB and, thus, corresponds to the whole range of possibly occurring *E*-vector orientations.

Because the *E*-vector map in the PB corresponds with the proposed output regions of the TB1 neurons, we asked whether candidate postsynaptic neurons show a similar representation of *E*-vector tuning. Columnar neurons have ar-

Animal Physiology, Department of Biology, Philipps University, 35032 Marburg, Germany.

*To whom correspondence should be addressed. E-mail: homberg@staff.uni-marburg.de

borizations in single columns of the PB and send axonal projections to an area outside the CC, the lateral accessory lobe (LAL). Several cell types have additional arborizations in distinct columns of the central body. Three types of these neurons are polarization-sensitive (Fig. 2). We evaluated the data from 19 recordings from these cell types, termed CPU1, CP1, and CP2 neurons. CPU1 neurons have smooth endings in single columns of the PB, in columns of the dorsalmost layer I of the upper division of the central body (CBU), and an axonal fiber with varicose endings in the LAL (Fig. 2A). Each neuron connects a single column of the PB with two neighboring columns of the CBU, following a wiring scheme described for *Drosophila* (*9*) (Fig. 2G). All CPU1 neurons (10 recordings) showed polarization opponency and background spiking activity of 20 to 40 Hz. Comparison of the innervated columns in the PB and Φ_{max} tuning again revealed a spatial representation of *E*-vector orientations across the PB, which covered a range of 228° ± 73° through the 8 PB columns in one brain hemisphere (Fig. 2I). The slope of the regression lines of TB1 and CPU1 neurons did not differ significantly [$P = 0.32$, analysis of covariance (*16*)], indicating that the tuning range through the 16 columns of the bridge matched for both cell types. However, the CPU1 map was shifted by 101° (equivalent to −79°) relative to the map of TB1 neurons (significantly different elevation of regression lines, $P < 0.0001$).

The remaining two types of columnar neurons, CP1 and CP2 neurons, also connected the PB with the LAL (Fig. 2, B, C, and H), but lacked arborizations in the central body. Within the LAL, projections were confined to either of two subcompartments, the median olive (CP1) or the lateral triangle (CP2). Both types of neuron had smooth arborizations in the PB and varicose endings in the LAL. In all recordings ($n = 9$), CP1 and CP2 neurons showed polarization opponency, but had lower background activity (3 to 15 Hz) than CPU1 and TB1 neurons. As for CPU1 and TB1 neurons, regression analysis of pooled data from CP1 and CP2 neurons revealed a linear correlation between the innervated column in the PB and the *E*-vector tuning of the neurons (Fig. 2J). The linear regression for CP1 and CP2 covered a range of 206° ± 76° over one hemisphere (eight columns) of the PB and was not significantly different from the linear regression for CPU1 neurons (slope: $P = 0.4777$, elevation: $P = 0.3525$). It was, however, phase-shifted by 111° (equivalent to −69°) against the map of TB1 neurons.

The present study shows, independently for three different cell types, that a map of zenithal *E*-vector orientations underlies the columnar organization of the locust PB. This spatial representation adds a level of complexity to sensory processing in the insect brain, hitherto thought to be achieved only in vertebrates. In most neurons at least half-maximal activation occurred over an *E*-vector orientation range of about 60°, implying considerable overlap for neighboring columns and the necessity of a population code for retrieving exact information from the firing rates of these cells (*17*).

Under the open sky, the activity in the POL neurons described here is directly related to the directional orientation of the locust's head, provided that additional mechanisms (color coding, intensity coding) allow the animal to distinguish the solar from the antisolar hemisphere of the sky. Color-coding properties suited to fulfill this requirement have been demonstrated recently for POL neurons at an input stage to the CC, the anterior optic tubercle (*18*). Neurons encoding head direction have been intensely studied in mammals (*19*, *20*). An important difference of the locust polarization analyzers in the CC is their global nature of signaling. The neurons fire according to zenithal *E*-vectors, which provide information about the Sun's azimuth and, therefore, these neurons behave like an internal 180° compass. In rats, in contrast, head-direction cells are recalibrated to visual landmarks in each new environment and are apparently not arranged topographically (*21*, *22*).

Although some progress has been made in analyzing the wiring principles from which computational maps arise in vertebrates (*23*, *24*), the simple brains of locusts offer the opportunity to address this question at the level of single identified neurons. Within the PB, the spatial maps of tangential and columnar neurons are out of phase by about 90°. If TB1 neurons are directly connected to the columnar neurons, a phase shift of 90° might most easily result from inhibitory connections of TB1 neurons to the dendritic

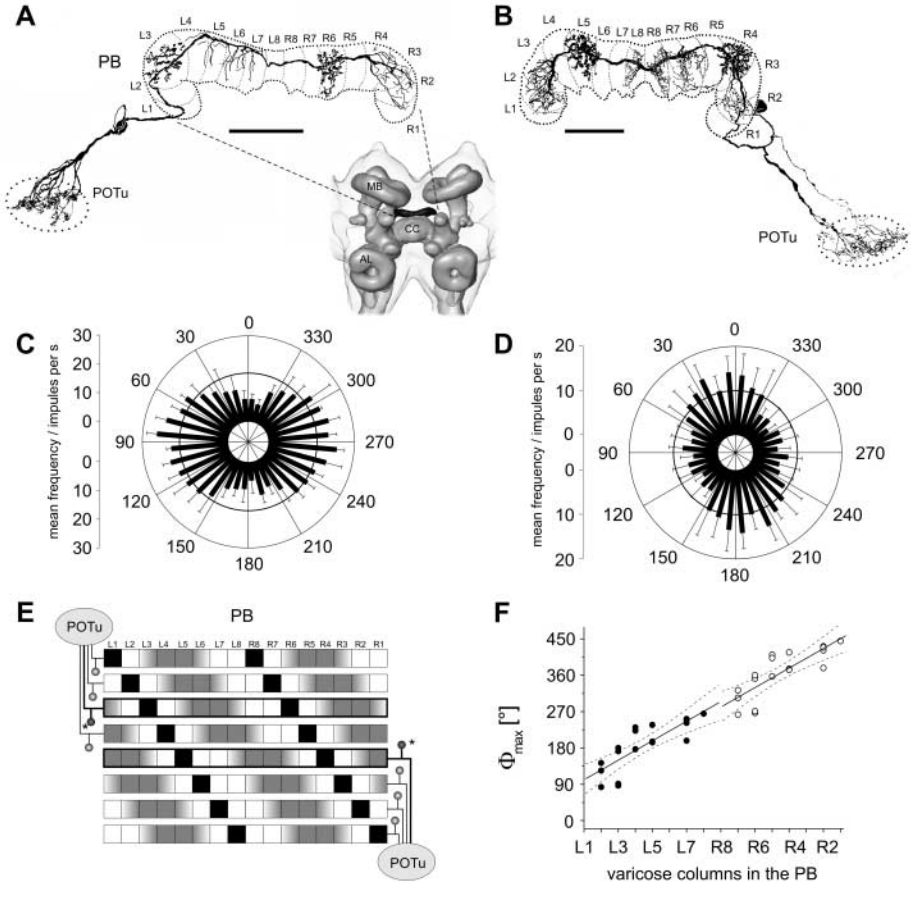

Fig. 1. Morphological and physiological properties of TB1 neurons. (**A** and **B**) Frontal reconstructions of two TB1 neurons; inset shows frontal view of the locust midbrain. Scale bars, 100 μm. (**C** and **D**) Circular plots of mean firing rate during *E*-vector rotations for the neuron in (A) [(C)] and (B) [(D)] ($n = 4$, bin width 10°; error bars: SD). Solid lines indicate background activity. (**E**) Wiring scheme of the TB1 neuron system. Each line represents one TB1 neuron in the PB (black squares: columns with varicose arborizations; gray squares: columns with smooth arborizations; white squares: columns without arborizations). Asterisks indicate TB1 neurons shown in (A) and (B). (**F**) Correlation between location of varicose columns in the PB and *E*-vector tuning (Φ_{max}) of TB1 neurons ($n = 18$). Because each neuron has varicose arborizations in single columns in the right and left PB hemisphere, Φ_{max} values were plotted twice for the right hemisphere (open circles) and the left hemisphere (filled circles). Linear regression shows significant correlation ($r = 0.81$, SD = 35.8°, $P < 0.0001$, two-tailed t test, $y = 24.2x + 77.0$). Also shown are 95% confidence bands (*13*). AL, antennal lobe; CC, central complex; MB, mushroom body; PB, protocerebral bridge; POTu, posterior optic tubercle.

trees of columnar neurons. Double-labeling experiments showed that serotonin and a Dip-allatostatin–related neuropeptide are present in TB1 neurons (fig. S5). For both substances, inhibitory effects have been demonstrated in other systems (*25*, *26*). Whereas azimuthal space is linearly represented in the columns of the PB, the wiring of CPU1 neurons should result in a superposition of the two 180° representations of the PB in the CBU, but with a lateral shift of about 50° (fig. S3). The functional consequences of this shift are presently unknown. If the *E*-vector tunings of corresponding CPU1 neurons in each of the eight double columns of the CBU are merged, the azimuth representation would be reduced to only about 156° of frontal space.

On the basis of the data presented here and a recent paper by Liu *et al*. (*12*), a coherent functional role for the CC is emerging. In *Drosophila*, tangential neurons innervating specific layers of the central body are essential for recognizing features of visual objects (elevation in the panorama; contour orientation). Columnar neurons, like the CPU1 neurons, are ideal candidates to associate these visual features with information on their azimuthal direction (fig. S4). Liu *et al*. (*12*) already hypothesized that the width of the CBU represents azimuthal space. This is strongly supported by our data, but this representation may differ between cell types and CC substructures as pointed out above.

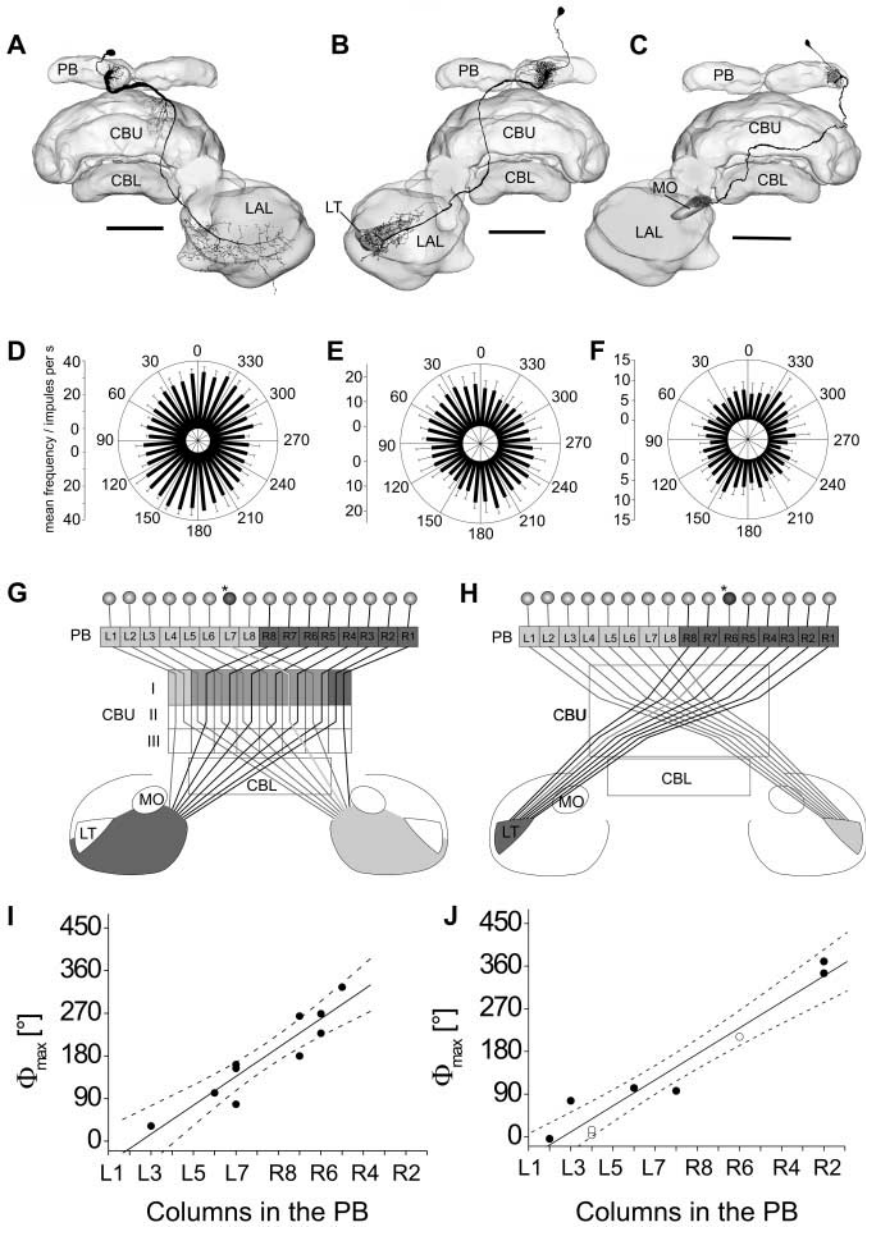

Fig. 2. Morphology and physiology of columnar neurons. (**A** to **C**) Camera lucida drawings of a CPU1 neuron (A), CP2 neuron (B), and CP1 neuron (C) projected onto three-dimensional reconstructions of the central complex. Scale bars, 100 μm. (**D** to **F**) Circular plots of mean firing rate during *E*-vector rotations for the neurons shown in (A) to (C) (n = 4, bin width 10°; error bars: SD). (**G** and **H**) Wiring schemes of the CPU1 neuron system and the CP2 neuron system. Asterisks indicate the CPU1 neuron shown in (A) [(G)] and the CP2 neuron shown in (B) [(H)]. The CP1 neuron system (not shown) projects to the MO but is otherwise identical to the CP2 system. (**I** and **J**) Linear correlation between the location of the columnar arborization domain in the PB and the *E*-vector tuning (Φ_{max}) of columnar neurons. (I) CPU1 neurons (r = 0.93, SD = 36.5°, P = 0.0001, two-tailed t test, $y = 30.4x - 76.2$). Midline crossing occurs at 182°. (J) CP1 neurons (open circles) and CP2 neurons (filled circles) have been combined for statistical analysis (r = 0.97, SD = 38.0°, $P < 0.0001$, two-tailed t test, $y = 27.4x - 61.8$). Midline crossing occurs at 171°. Confidence bands are shown at 95%. CBL, CBU, lower and upper divisions of the central body; LAL, lateral accessory lobe; LT, lateral triangle; MO, median olive; PB, protocerebral bridge.

References and Notes

1. R. Wehner, *J. Exp. Biol.* **204**, 2589 (2001).
2. G. Horváth, D. Varjú, *Polarized Light in Animal Vision: Polarization Patterns in Nature* (Springer, Berlin, 2004).
3. M. Mappes, U. Homberg, *J. Comp. Physiol. A* **190**, 61 (2004).
4. M. Mappes, U. Homberg, *J. Comp. Physiol. A* **193**, 43 (2007).
5. H. Vitzthum, M. Müller, U. Homberg, *J. Neurosci.* **22**, 1114 (2002).
6. U. Homberg, S. Hofer, K. Pfeiffer, S. Gebhardt, *J. Comp. Neurol.* **462**, 415 (2003).
7. K. Pfeiffer, M. Kinoshita, U. Homberg, *J. Neurophysiol.* **94**, 3903 (2005).
8. J. L. D. Williams, *J. Zool. London* **176**, 67 (1975).
9. U. Hanesch, K. F. Fischbach, M. Heisenberg, *Cell Tissue Res.* **257**, 343 (1989).
10. M. Müller, U. Homberg, A. Kühn, *Cell Tissue Res.* **288**, 159 (1997).
11. R. Strauss, *Curr. Opin. Neurobiol.* **12**, 633 (2002).
12. G. Liu *et al.*, *Nature* **439**, 551 (2006).
13. Material and methods are available as supporting material on *Science* Online.
14. U. Homberg, S. Würden, *J. Comp. Neurol.* **386**, 329 (1997).
15. E. Batschelet, *Circular Statistics in Biology* (Academic Press, London, 1981).
16. J. Zar, *Biostatistical Analysis* (Prentice-Hall, Englewood Cliffs, NJ, 1999).
17. E. I. Knudsen, S. du Lac, S. Esterly, *Annu. Rev. Neurosci.* **10**, 41 (1987).
18. K. Pfeiffer, M. Kinoshita, U. Homberg, *Proceedings of the 6th Meeting of the German Neuroscience Society* (www.neuroanatomie.uni-goettingen.de/neurobio_archiv/2005/pdf/Proceedings-Goettingen2005.pdf), p. 218.
19. P. E. Sharp, H. T. Blair, J. Cho, *Trends Neurosci.* **24**, 289 (2001).
20. J. S. Taube, J. P. Bassett, *Cereb. Cortex* **13**, 1162 (2003).
21. F. Sargolini *et al.*, *Science* **312**, 758 (2006).
22. H. Mittelstaedt, *Biol. Cybern.* **83**, 261 (2000).
23. H. J. Chisum, D. Fitzpatrick, *Neural Netw.* **17**, 681 (2004).
24. F. Mooser, W. H. Bosking, D. Fitzpatrick, *Nat. Neurosci.* **7**, 872 (2004).
25. W. Blenau, A. Baumann, *Arch. Insect Biochem. Physiol.* **48**, 13 (2001).
26. E. M. Tan *et al.*, *Neuron* **51**, 157 (2006).

27. We thank S. Gebhardt, S. Gotthardt, K. Pfeiffer, and H. Vitzthum for contributing physiological data; K. Pfeiffer for help with data evaluation; A. Kurylas for providing three-dimensional reconstructions of brain structures; and E. Buchner for providing the antibody to synapsin. This work was supported by the Deutsche Forschungsgemeinschaft (grants HO 950/14-3 and HO 950/16-1).

Supporting Online Material

www.sciencemag.org/cgi/content/full/315/5814/995/DC1
Material and Methods
Figs. S1 to S5
References

25 September 2006; accepted 4 January 2007
10.1126/science.1135531

Supporting Online Material for

Maplike Representation of Celestial *E*-Vector Orientations in the Brain of an Insect

Stanley Heinze and Uwe Homberg*

*To whom correspondence should be addressed. E-mail: homberg@staff.uni-marburg.de

Published 16 February 2007, *Science* **315**, 995 (2007)
DOI: 10.1126/science.1135531

This PDF file includes:

Science **Supporting online material**

Map-like representation of celestial *E*-vector orientations in the brain of an insect

Stanley Heinze & Uwe Homberg

Animal Physiology, Department of Biology, Philipps University, 35032 Marburg, Germany

Contents

Material and Methods

Animals.

Experiments were performed on 37 adult desert locusts (*Schistocerca gregaria*) of both sexes from a crowded laboratory colony. Locusts were waxed to a holder as described (S1). After removal of the legs and wings, the head was opened frontally and the brain was exposed. The brain was supported from posterior with a small metal platform that also served as indifferent electrode. To allow penetration of the recording electrode, the neurilem was mechanically removed. During recording the brain was constantly bathed in locust saline (S2).

Visual stimuli.

Visual stimuli were produced by passing light from a xenon arc (XBO 150 W) through a standard glass light guide and a rotating polarizer. Stimuli were presented from the zenith, had an irradiance of 94 μW/m², and appeared at an angular size of 2.7°. For testing polarization sensitivity the polarizer was rotated through 360° (in one experiment 180°) in both directions with an angular velocity of 21°/s.

Electrophysiology.

Microelectrodes (resistance: 60 – 150 MΩ) were drawn from borosilicate capillaries. Their tips were filled with 4% Neurobiotin in 1 M KCl and backed up with 1 M KCl. Signals were amplified (10x) with a custom-built amplifier, sampled at 25 kHz with a Digidata 1322A, and stored on a personal computer using pClamp9. After recording, Neurobiotin was injected iontophoretically into the recorded neuron with a constant depolarizing current (3 nA, 1 - 2 min).

Histology.

After recording, brains were dissected out of the animals, fixed over night at 4° C, and incubated for three days with Cy3-conjugated Streptavidin at a concentration of 1:1000. Brains were dehydrated in ethanol, cleared in methylsalicylate, and mounted in Permount between coverslides. For detailed analysis, preparations were rehydrated in a decreasing ethanol series, embedded in albumin/gelatine, sectioned at 40 μm with a vibrating blade microtome, and incubated with Streptavidin conjugated with horseradish peroxidase (1:200), followed by staining with 3,3'-diaminobenzidine tetrahydrochloride (DAB) as described by Vitzthum et al. (S3). DAB-stained neurons were reconstructed using a light microscope with camera lucida attachment. Three-dimensional reconstructions of the locust brain were performed with Amira3.1. Image stacks were obtained using a confocal microscope. Detailed images of the central complex were scanned from thick slice preparations (200 μm, 20x objective) immunolabelled with anti-synapsin (kindly provided by E. Buchner, University of Würzburg, Germany). Whole brain reconstructions were

obtained from wholemount preparations (10x objective) immunolabelled with anti-synapsin. For visualization of neuronal ramifications, 3D-reconstructions and camera lucida reconstructions were projected onto each other.

Evaluation of morphologies.

To determine the identity of innervated columns, we evaluated the boundaries of the PB with differential interference contrast optics (DAB-stained preparations), anti-synapsin-staining (Cy3-fluorescent preparations with anti-synapsin counterstaining), or unspecific background staining. As neighboring columns are not separated by visible structures, their individual identity was inferred from the location of the brain midline, the overall length of the PB, and the exit sites of major axonal tracts projecting from the PB to the CBU.

Data analysis.

Spike trains were analysed with custom-designed scripts in Spike2-software. Relative times of action potentials were evaluated with a threshold-based detection algorithm. During stimulation with the rotating polarizer, each spike was assigned to its corresponding *E*-vector angle. Neurons were regarded as polarization-sensitive if the distribution of these *E*-vector angles differed significantly from randomness (Rayleigh test for axial data (S4); $\alpha = 0.05$, software Oriana 2.0). The mean vector of the distribution was defined as the preferred *E*-vector orientation (Φ_{max}) of that neuron.

E-vector orientations (Φ_{max}-values) are bidirectional axial data with a periodicity of 180° and can, therefore, be plotted from 0°-180° or from 180°-360°. In a first step of analysis of the spatial representation of *E*-vector tuning of columnar neurons we consequently plotted each Φ_{max}-value twice, as x (ranging from 0°-180°) and as x+180° (ranging from 180°-360°) against their columnar arborization domains (Fig. S1). This led to three approximately linear and parallel bands of data points and, thus, suggests a linear correlation between Φ_{max}-values and columnar arborization domains throughout the 16 columns of the PB. For a statistical analysis of the data, Φ_{max}-values from neurons with arborizations in the left hemisphere were, therefore, plotted in the range from 0°-180° and

Φ_{max}-values from neurons with arborizations in the right hemisphere in the range from 180°-360°.

As TB1-neurons have one varicose columnar arborization domain in each hemisphere of the PB, only the data covering one hemisphere were evaluated statistically. Because of the morphology of these neurons (varicose columns are strictly 8 columns apart from each other) data points for the second hemisphere of the bridge are identical to those of the first one. Hence the 180°-shift for the right hemisphere in Fig. 1F has been performed to provide easier comprehensiveness and the same format as used in Fig. 2. Analysis of linear correlation between the columnar arborization domains of the neurons and their Φ_{max}-values was performed with the linear fit tool in Origin 6.0. It calculated the correlation coefficient r, the 95% confidence bands and performed a two-tailed t-test. The confidence bands indicate that at an α-level of 0.05 the mean y-values (here Φ_{max}) for any given x-value (here columns or relative distance) lie within the confidence bands. The correlation was rated significantly different from 0 if the p-value of the t-test was below the significance level of 0.05. The resulting regression line was used to calculate the *E*-vector range of one PB hemisphere and the intersection point with the brain midline. Phase-shifts between different functions were determined at the intersection with the brain midline. Doubled standard deviations are indicated as errors of the *E*-vector-range for each regression function.

The residues of each linear regression were tested for normality with the Shapiro-Wilk-Test (performed with XLSTAT 2006 Version 2006.2). The test is regarded as the most reliable test for non-normality for small to medium sample sizes (S5). No significant indications of non-normality could be found for any neuron type (p-values: TB1: 0.262, CPU1: 0.140, CP: 0.903). Regression lines of different neuron types were compared using GraphPadPrism4.0. The resulting (two-tailed) p-values were derived from a method equivalent to ANCOVA analysis as described (S6). The slopes and intercepts of two regression lines were rated significantly different if p-values were below 0.05.

To test for the reliability of column identification, we evaluated the position of the arborizations with a second method. We measured the distance of arborization centers from the midline (summed distance in XY- and Z-direction) and normalized these distances

for the total length of the PB. These values were plotted with respect to the left end of the PB (left end, 0; midline, 0.5; right end, 1; shown in Fig. S2). Comparison with the columnar plots (Figs. 1, 2) show that both methods provide virtually identical results. For comparison of the slopes of the linear regressions with those in Figs. 1 and 2, slope values of Fig. S2 have to be divided by 15, because x-values in Figs 1 and 2 range from 1-16.

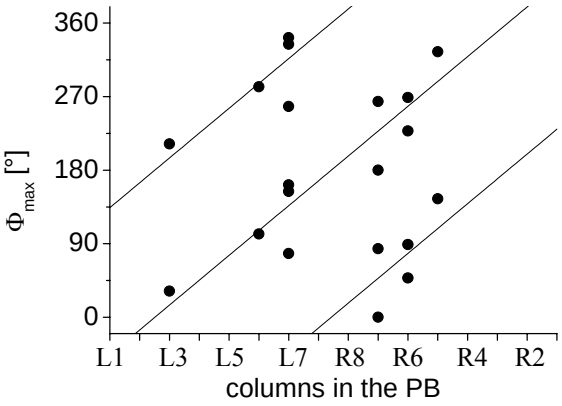

Fig. S1. Correlation between Φ_{max}–values and columnar arborizations of CPU1-neurons. Each data point is plotted twice, first in the range of 0°-180° and second in the range of 180°-360°, as described in the supplementary methods. Superimposed on the data is the linear regression line obtained from one complete dataset plus the corresponding lines shifted by ±180° (equation: y = 30.4x – 76.2).

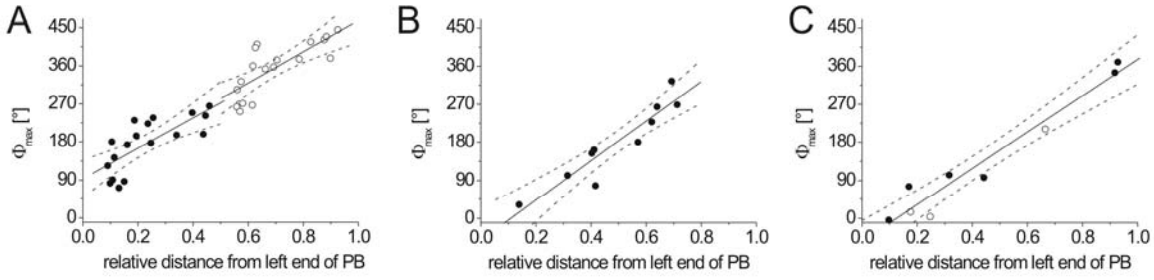

Fig. S2. Linear correlations between *E*-vector tuning (Φ_{max}) and relative distance of columnar arborization from the left end of the protocerebral bridge. **(A)** TB1-neurons. Details for left hemisphere: r = 0.75, SD = 42.7°, p < 0.001, two-tailed t-test, y = 358.9x + 93.0. Right hemisphere: r = 0.77, SD = 40.7, p < 0.001, y = 369.6x + 97.4. **(B)** CPU1-neurons: r = 0.93, SD = 35.2, p < 0.0001, y = 468x - 50.7. Midline crossing occurs at 183.3°. **(C)** CP-neurons (filled circles, CP1-neurons; open circles, CP2-neurons): r = 0.97, SD = 35.3, p < 0.0001, y = 429.8x - 53.8. Midline crossing occurs at 161.1°. Confidence bands are shown at 95%.

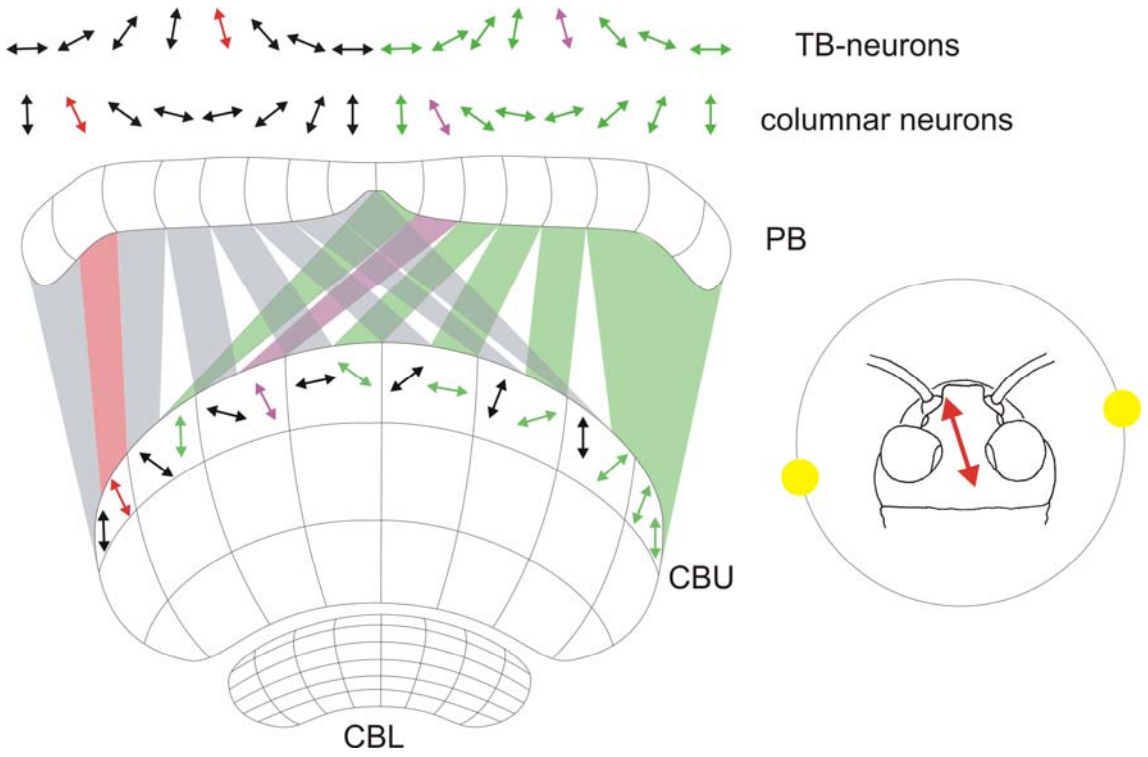

Fig. S3. Summary of the main findings of the paper. *E*-vector orientations of polarized light, shown to the animal from the zenith, are represented in a topographical manner within the columns of the protocerebral bridge (PB). Neurons with ramifications in a particular column respond maximally to a certain *E*-vector. Over the range of the PB each possibly ocurring *E*-vector is represented twice, with neighboring columns differing by an angle of approximately 26°. The maps of TB-neurons and columnar neurons are out of phase by about 90°, which means that at any given stimulus situation the column with maximal activity for TB1-neurons corresponds to the column with minimal activity for columnar neurons. The columnar map is projected onto the upper unit of the central body (CBU) by columnar CPU1-neurons. Here the twofold representation of the PB is superimposed and shifted laterally by about 50°. When the locust is stimulated with a certain *E*-vector (right side), it follows that activity is highest in the highlighted (red and violet) columns of the central complex. This enables the animal to determine the direction it faces relative to the sun, as long as the solar and antisolar side of the sky can be determined by other means.

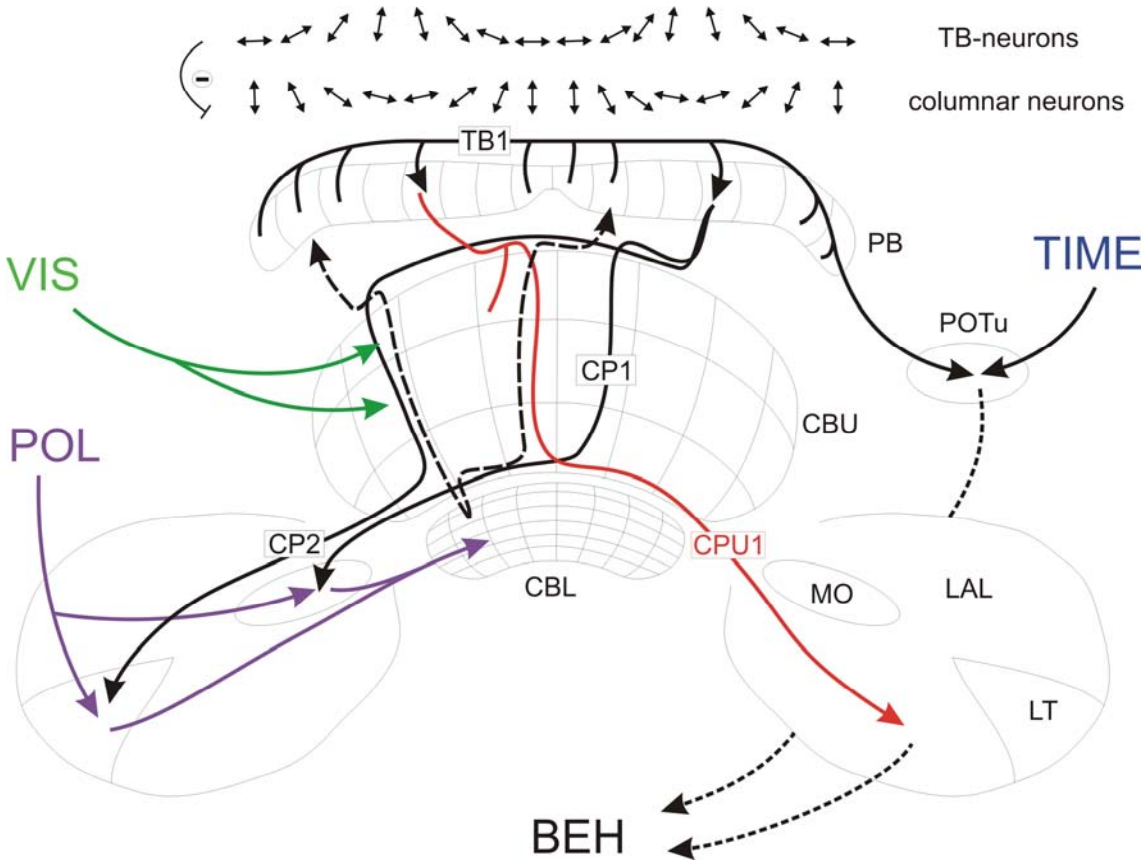

Fig. S4. Proposed network of the central complex in the locust. Two computational maps of *E*-vector orientations are present in the columns of the PB. As both maps cover the same range but are out of phase by about 90°, an inhibitory connection between TB1 and columnar neurons is most likely. When the animal is stimulated with a certain *E*-vector (e.g. the one highlighted) neurons of a single column in each hemisphere are maximally activated in each map. Although it is not clear how these maps are generated within the brain, we can put forward the general outline of a possible wiring scheme of the POL-network in the central complex. Polarized-light information enters the central complex via the medial olive (MO) and the lateral triangle (LT) (S1) and is further relayed to the lower division of the central body (CBL) (S3). It is not known how *E*-vector information enters the PB, but we postulate a connection between the CBL and the PB (dashed lines). TB1-neurons integrate *E*-vector information from several columns and transmit it further to feedback loops (CP1 and CP2-neurons) and to CPU1 neurons. CPU1 neurons (red) are suited to integrate visual information present in the layers of the CBU (VIS, green) (S7), and thus provide one of several outputs of the central complex to the LAL. Together with a possible output pathway from the posterior optic tubercle (POTu), information is finally transferred to descending neurons that guide behaviour (BEH). Inputs from the proposed circadian clock (accessory medulla, TIME) to the POTu (S8) point to a possible time compensation pathway. For simplification only neurons connected with one TB1-neuron are shown. Input neurons are shown only for the left hemisphere and proposed output connections are shown for the right hemisphere only.

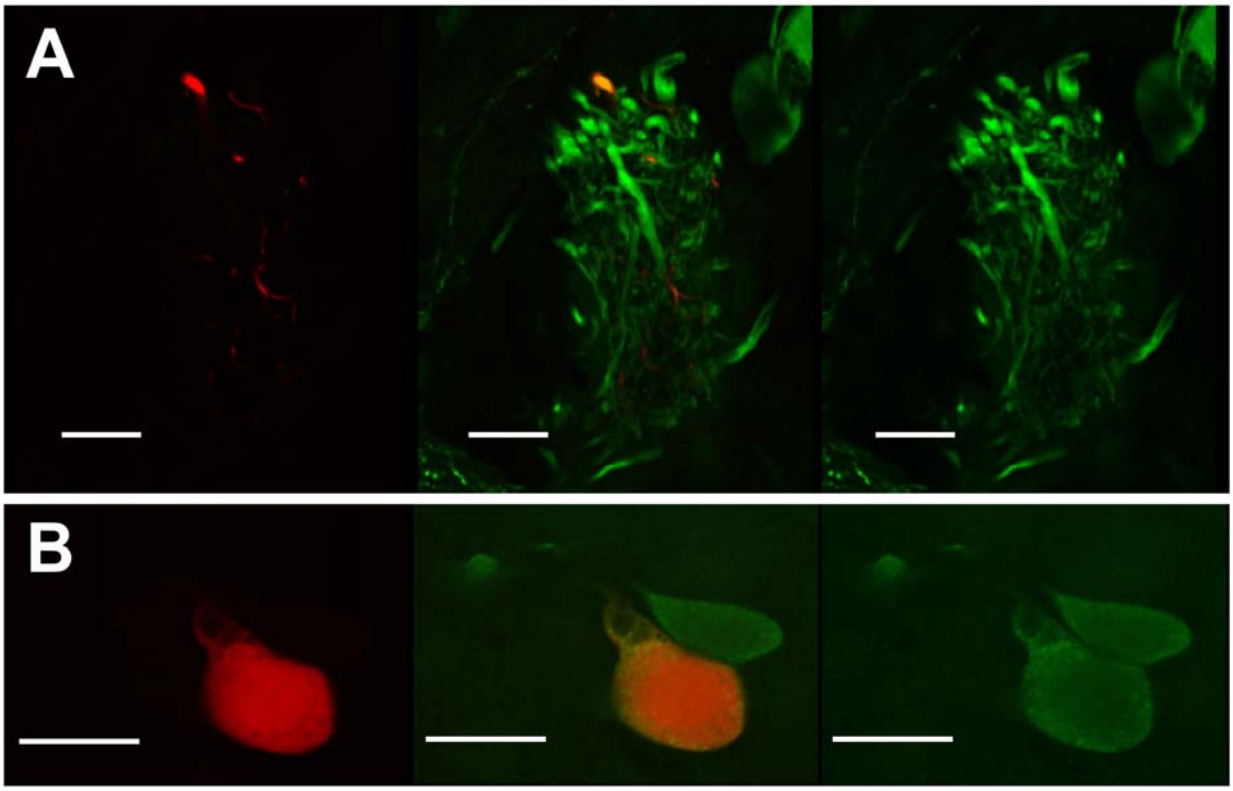

Fig. S5. Demonstration of serotonin immunostaining (green fluorescence; rabbit anti-serotonin, detected with Cy2-conjugated goat-anti-rabitt) in a TB1-neuron (red fluorescence, Neurobiotin-injected, Cy3-conjugated Streptavidin). Single frontal optical sections (0.5 µm) from confocal image stacks. **(A)** Colabelling in tangential projections within the protocerebral bridge. **(B)** Double-labelled soma of the injected neuron. Scale bars, 20µm. All serotonin-immunoreactive TB1-neurons are also Dip-allatostatin-immunoreactive (S9).

References

S1. K. Pfeiffer, M. Kinoshita, U. Homberg, *J. Neurophysiol.* **94**, 3903 (2005).

S2. A. Clements, T. May, *J. Exp. Biol.* **60**, 673 (1974).

S3. H. Vitzthum, M. Müller, U. Homberg, *J. Neurosci.* **22**, 1114 (2002).

S4. E. Batschelet, *Circular Statistics in Biology*. (Academic Press, London, 1981).

S5. W. J. Conover, *Practical Nonparametric Statistics*, (Wiley, 1999).

S6. J. Zar, *Biostatistical Analysis*. (Prentice Hall, 1999).

S7. G. Liu *et al*., *Nature* **439**, 551 (2006).

S8. U. Homberg, S. Würden, *J. Comp. Neurol.* **386**, 329 (1997).

S9. H. Vitzthum, U. Homberg, H. Agricola, *J. Comp. Neurol.* **369**, 419 (1996).